Second-order susceptibility of $Ga_{0.5}In_{0.5}P$ crystals at 1.5 μm and their feasibility for waveguide quasi-phase matching

Yoshiyasu Ueno,* Vincent Ricci, and George I. Stegeman

Center for Research and Education in Optics and Lasers, University of Central Florida, 4000 Central Florida Boulevard, Orlando, Florida 32816-2700

Received April 29, 1996; revised manuscript received September 19, 1996

The second-order susceptibilities (d_{ij}) of both ordered and disordered $Ga_{0.5}In_{0.5}P$ semiconductor crystal films epitaxially grown on GaAs substrates are analyzed. Quasi-phase matching based on periodic order–disorder regions is proposed, and the analysis shows that three of the four independent coefficients, namely, d'_{33}, d'_{31}, and d'_{15}, but not d'_{14}, can be modulated. Maker-fringe experiments were performed at 1.57 μm to measure these coefficients in the deposited crystals. However, the crystal-film orientation allowed a definitive determination of the d'_{14} coefficient (110 pm/V) only and an upper limit of 60 pm/V for d'_{33}. More-sophisticated experimental techniques are proposed for measuring d'_{33}. © 1997 Optical Society of America [S0740-3224(97)03906-4]

1. INTRODUCTION

Nonlinear $\chi^{(2)}$ materials are attracting new attention for ultrafast all-optical switches based on the $\chi^{(2)}$:$\chi^{(2)}$ cascading mechanism.[1,2] Recent experiments and analyses with KTP (d_{33} = 18.5 pm/V)[3] and $LiNbO_3$ (d_{31} = 5.6 pm/V)[4] have shown the potential of cascading to decrease the switching power to a practical level. Another relevant optical device based on $\chi^{(2)}$ is an optical parametric oscillator, which has been demonstrated with $LiNbO_3$ (d_{33} equals 30–40 pm/V).[5] For both devices, phase matching as well as a large $\chi^{(2)}$ are the key material requirements. Although semiconductors have large nonresonant $\chi^{(2)}$ values (e.g., d_{14} equals 90–130 pm/V, that is, $\chi^{(2)}_{xyz}$ equals $4-6 \times 10^{-7}$ esu for GaAs[6]), the necessary phase-matching conditions have been difficult to achieve. To date, two AlGaAs waveguide structures have been proposed for quasi-phase matching (QPM) in semiconductors; one is an asymmetric-quantum-well structure,[7] and the other is a domain-inverted structure fabricated by wafer bonding.[8]

A $Ga_{0.5}In_{0.5}P$ crystal [more generally, $(Al_xGa_{1-x})_yIn_{1-y}P$ crystals], when grown on a GaAs substrate, has a unique structure among inorganic materials. As shown in Fig. 1, Ga-rich planes ($Ga_{0.5+\delta}In_{0.5-\delta}$) and In-rich planes ($Ga_{0.5-\delta}In_{0.5+\delta}$) alternate in the $[\bar{1}, 1, 1]$ (or $[1, \bar{1}, 1]$) direction. The crystal symmetry is $C_{3v}(3m)$. Because this structure was first observed as super spots in transmission-electron-microscope images for epitaxial GaInP and AlGaInP crystals grown on GaAs substrates by metallorganic vapor phase epitaxy, it has been sometimes called an ordering or natural superlattice.[9] It has been shown that the ordered structure is formed under a wide range of growth temperatures. It has also been proven that this crystal is stable; for example, red-laser diodes in which GaInP ordered crystals were used as the active layer have exhibited stable operation for thousands of hours at 50 °C.[10] Along with intensive research on crystal growth and red lasers (λ_L equals 0.6–0.7 μm), many of the linear properties such as refractive-index dispersion,[11] anisotropic band structure,[12] and anisotropic oscillator strengths[12,13] have been reported. Although the birefringence has not been measured directly, its existence was recently suggested from studies of waveguide modes.[14] With the exception of two-photon absorption (TPA) at 0.88 μm,[15] the nonlinear susceptibilities have not been reported to date to our knowledge.

Under certain growth conditions, epitaxial GaInP crystals do not exhibit the ordered structure in which the Ga and In atoms are randomly located (i.e., $\delta = 0$) on the group III sites, in contrast to Fig. 1. Consequently the crystal structure is zinc blende, the same structure as GaAs. Not only growing either of the two crystal structures by using a specific growth condition, we can also change the one structure into the other one after the crystal growth. Impurity, diffused or implanted into an ordered GaInP crystal after the growth, changes the ordered structure to a disordered one.[16] Selective-area disordering obtained by a patterned mask has readily been demonstrated for lasers.[16] Disordering techniques are similar to those well studied for quantum-well disordering, except for the significant difference that the order period of 0.65 nm for GaInP is much shorter than that for quantum wells (typically ~10 nm).

In this paper we examine the $\chi^{(2)}$ properties of GaInP crystals for potential application to order–disorder quasi-phase-matched waveguides useful for efficient operation of all-optical devices at 1.5 μm.[17] After comparing the nonlinear d_{ij} matrices of ordered and disordered GaInP in Section 2, we show an example of a possible order–disorder-type quasi-phase-matched waveguide in Section 3 and analyze the nonlinearities appropriate to guided modes. In addition to the potential for QPM, this crystal

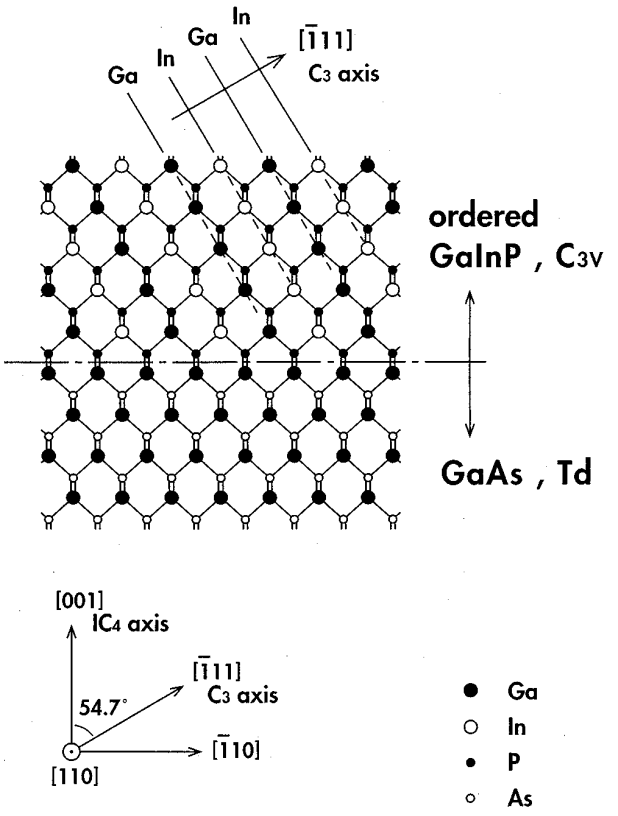

Fig. 1. Ordered $Ga_{0.5}In_{0.5}P$ crystal grown on GaAs.[9] The crystal symmetry is C_{3v}. The $[\bar{1}, 1, 1]$ symmetry axis is tilted 54.7° from the [0, 0, 1] growth direction. The band-gap energy is 1.8–1.9 eV, which is more than twice as large as the 1.55-μm photon energy of 0.8 eV.

has other advantages as a $\chi^{(2)}$ material for 1.5-μm applications. The band-gap energy (1.8–1.9 eV), as compared with GaAs (1.45 eV), should be sufficiently large to suppress any TPA at 1.5 μm (photon energy 0.8 eV). On the other hand, the 1.5-μm photon energy is close enough to half the band gap that the d_{ij} coefficients should be resonantly enhanced, as predicted theoretically by Ghahramani and Sipe for zinc blende ZnSe.[18] In addition, the C_{3v} symmetry of this crystal allows permanent dipoles, which would further enhance the coefficients near resonance. The photon energy is much closer to half the GaInP band-gap energy from below, compared with that of ZnSe or ferroelectric crystals such as $LiNbO_3$. More important from a practical perspective, the processing techniques required for fabricating order–disorder waveguides would have more design flexibility and would be more reproducible than previously reported for AlGaAs.

We attempted to use Maker-fringe techniques to measure the four independent d_{ij} coefficients of GaInP, using thin-film samples grown on GaAs substrates. In principle it is possible to obtain these coefficients from a simple analysis, as will be shown in Section 4. However, during the measurements we found that three factors combined to prevent us from measuring the d'_{33} and d'_{31} coefficients that can be modulated by disordering. They are the disadvantageous orientation (for Maker-fringe measurements) of the crystal film relative to the substrate; the limited range, owing to the high semiconductor refractive indices, of internal incidence angles for the fundamental beam; and, for such small internal angles of incidence, the dominance of the second-harmonic-generation (SHG) signal by the d'_{14} coefficient (measured to be 110 pm/V, not affected by disordering). This resulted in an experimental upper limit of approximately 60 pm/V for the d'_{33} coefficient, corresponding to $<1°$ misalignment in the polarizers, as shown in Section 5, with experimental and calculated data. Other possible but more-sophisticated measurement techniques to evaluate these coefficients are briefly discussed. Section 6 summarizes this study.

2. NONLINEAR d_{ij} MATRICES

First, the d_{ij} matrices for the ordered (Fig. 1) and disordered crystals are discussed and compared. Second, a correction appropriate to a domain mixture is discussed.

Because the crystal symmetry of the ordered GaInP crystal is C_{3v}, it should have a d_{ij} matrix of the form[19]

$$d_{ij}^{(\mathrm{O}:C_{3v})} = \begin{bmatrix} 0 & 0 & 0 & 0 & d_{15} & -d_{22} \\ -d_{22} & d_{22} & 0 & d_{15} & 0 & 0 \\ d_{31} & d_{31} & d_{33} & 0 & 0 & 0 \end{bmatrix}, \quad (1)$$

where $(\mathrm{O}:C_{3v})$ stands for an ordered crystal in the C_{3v} frame of reference, i.e., [1, 1, 0], $[\bar{1}, 1, \bar{2}]$, and $[\bar{1}, 1, 1]$ are the principal axes in Fig. 1. In contrast, the symmetry for the counterpart, a disordered GaInP crystal, is zinc blende T_d $(\bar{4}3m)$, whose d_{ij} matrix has the form

$$d_{ij}^{(\mathrm{DO}:T_d)} = \begin{bmatrix} 0 & 0 & 0 & d''_{14} & 0 & 0 \\ 0 & 0 & 0 & 0 & d''_{14} & 0 \\ 0 & 0 & 0 & 0 & 0 & d''_{14} \end{bmatrix}, \quad (2)$$

where $(\mathrm{DO}:T_d)$ stands for a disordered crystal in the T_d frame of reference ([1, 0, 0], [0, 1, 0], and [0, 0, 1] are the principal axes). Since the C_{3v} axis is tilted by 54.7° from one of the T_d axes, we transformed the $d_{ij}^{(\mathrm{O}:C_{3v})}$ matrix into the T_d frame for comparison:

$$d_{ij}^{(\mathrm{O}:T_d)} = \begin{bmatrix} -d'_{33} & -d'_{31} & -d'_{31} & d'_{14} & d'_{15} & d'_{15} \\ d'_{31} & d'_{33} & d'_{31} & d'_{15} & d'_{14} & -d'_{15} \\ d'_{31} & d'_{31} & d'_{33} & d'_{15} & -d'_{15} & d'_{14} \end{bmatrix}, \quad (3)$$

where the d_{ij} components are relabeled as d'_{ij} for simplicity. The d'_{ij} coefficients are linearly related to the original d_{ij} coefficients by

$$\begin{bmatrix} d'_{33} \\ d'_{31} \\ d'_{14} \\ d'_{15} \end{bmatrix} = \frac{\sqrt{3}}{9} \begin{bmatrix} 4d_{15} + d_{33} - 2\sqrt{2}d_{22} + 2d_{31} \\ -2d_{15} + d_{33} + \sqrt{2}d_{22} + 2d_{31} \\ 2d_{15} - d_{33} + 2\sqrt{2}d_{22} + d_{31} \\ d_{15} + d_{33} + \sqrt{2}d_{22} - d_{31} \end{bmatrix}$$

$$\approx \begin{bmatrix} 0.77d_{15} + 0.19d_{33} - 0.54d_{22} + 0.38d_{31} \\ -0.38d_{15} + 0.19d_{33} + 0.27d_{22} + 0.38d_{31} \\ 0.38d_{15} - 0.19d_{33} + 0.54d_{22} + 0.19d_{31} \\ 0.19d_{15} + 0.19d_{33} + 0.27d_{22} - 0.19d_{31} \end{bmatrix}. \quad (4)$$

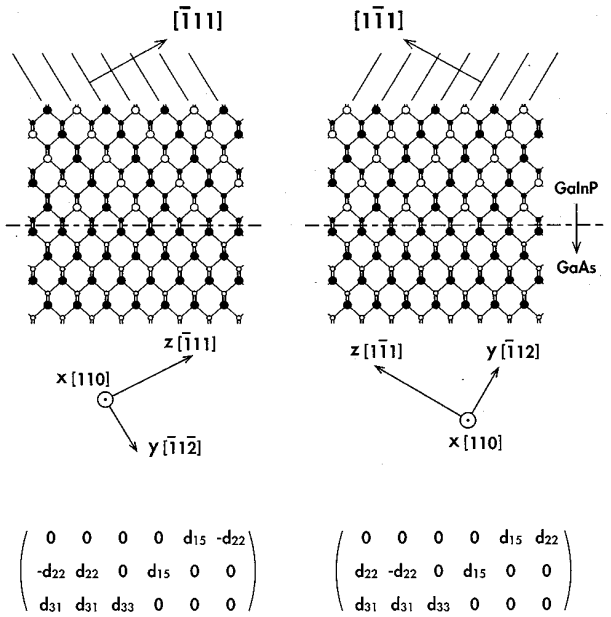

Fig. 2. Two equivalent domains of $Ga_{0.5}In_{0.5}P$ grown on a (0, 0, 1) GaAs substrate.[22,23]

The $d_{ij}^{(O:T_d)}$ in Eq. (3) has d'_{14} components in a manner similar to the T_d-symmetric $d_{ij}^{(DO:T_d)}$ in Eq. (2). This is because the $C_{3\nu}$ symmetry group is a subgroup of T_d.[20]

A comparison between the matrices of the ordered ($d_{ij}^{(O:T_d)}$) and disordered ($d_{ij}^{(DO:T_d)}$) lattices in the same frame of reference gives valuable insight. First, one finds that the d'_{33}, d'_{31}, and d'_{15} coefficients are physically related to the $C_{3\nu}$ distortion of this material in contrast to the d'_{14}, which is not, and whose origin is in the original noncentrosymmetric T_d structure. We suggest that the 7% difference between the lattice constants of GaP (5.45 Å) and InP (5.87 Å) implies a large $C_{3\nu}$ distortion and thus a large perturbation for each $C_{3\nu}$-related coefficient. The strong localization of electron states reported by Kurimoto and Hamada[21] also implies a large perturbation for each $C_{3\nu}$-related coefficient, when compared with the d'_{14} coefficient, which should be relatively unaffected and, consequently, similar to that of GaAs (of order 90–130 pm/V).[6]

Second, the effect of a domain mixture (Fig. 2) was taken into account. Ordered GaInP crystals, when grown on (0, 0, 1) surfaces, contain both [$\bar{1}$, 1, 1]- and [1, $\bar{1}$, 1]-oriented domains.[22,23] Because the domain size is supposed to be much smaller than an optical wavelength in the crystal, we can assume that the light field experiences the average of the d_{ij} matrices for the [$\bar{1}$, 1, 1]- and [1, $\bar{1}$, 1]-oriented domains. Although the average over the respective domains cancels out some components in the $d_{ij}^{(O:Td)}$ matrix in Eq. (3), i.e.,

$$d_{ij}^{(Mix:T_d)} = \begin{bmatrix} 0 & 0 & 0 & d'_{14} & d'_{15} & 0 \\ 0 & 0 & 0 & d'_{15} & d'_{14} & 0 \\ d'_{31} & d'_{31} & d'_{33} & 0 & 0 & d'_{14} \end{bmatrix}, \quad (5)$$

some of the $C_{3\nu}$-related components remain the same. The resultant $d_{ij}^{(Mix:Td)}$ is a $C_{2\nu}$-type d_{ij} matrix, which should correspond reasonably well to the macroscopic crystal symmetry of the domain-mixed ordered GaInP.[24] Note that when the matrix for the [1, $\bar{1}$, 1]-oriented domain is defined in its own $C_{3\nu}$ frame of reference (axes [1, 1, 0], [$\bar{1}$, 1, 2], and [1, $\bar{1}$, 1]), i.e.,

$$d_{ij}^{(O:\overline{C_{3\nu}})} = \begin{bmatrix} 0 & 0 & 0 & 0 & d_{15} & d_{22} \\ d_{22} & -d_{22} & 0 & d_{15} & 0 & 0 \\ d_{31} & d_{31} & d_{33} & 0 & 0 & 0 \end{bmatrix}, \quad (6)$$

the signs of the d_{22} components must differ from those of the initial d_{22} in $d_{ij}^{(O:C_{3\nu})}$ as in Eq. (1). This is because the [1, $\bar{1}$, 1]-oriented lattice is inverted with respect to the [$\bar{1}$, 1, 1]-oriented lattice.

3. QUASI-PHASE-MATCHED GEOMETRIES

It is shown next that this material has potential for QPM. Figure 3 shows a possible quasi-phase-matched waveguide structure. An area-selective disordering process by impurity implantation or diffusion can be used to periodically modulate the d_{ij} matrix between the $d_{ij}^{(Mix:Td)}$ and $d_{ij}^{(DO:Td)}$ discussed in Section 2, and this modulation in the d_{ij} components can be used to phase match the fundamental and the second-harmonic (SH) waves. The disordering process can be done either before or after fabricating the channel.

Quasi-phase-matched geometries were examined for conventional (0, 0, 1) waveguide geometries that have ($\bar{1}$, 1, 0) or (1, 1, 0) cleaved facets. A TE mode is polarized along [1, 1, 0] (or [$\bar{1}$, 1, 0]), and the TM mode is polarized along [0, 0, 1]. The optical fields experience a modulation of the d_{ij} matrices when traversing the ordered- and the disordered-crystal regions, given by

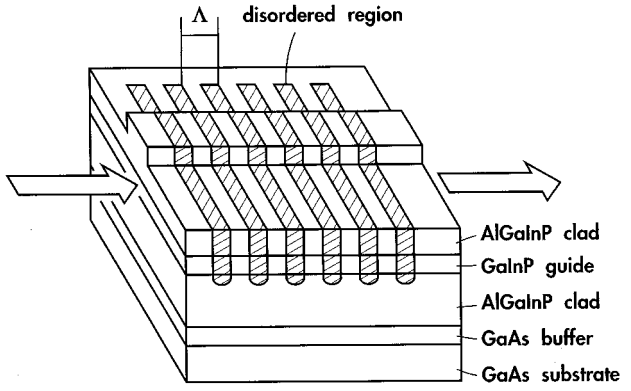

Fig. 3. Possible quasi-phase-matched waveguide structure using an AlGaInP–GaInP–AlGaInP double heterostructure. Area-selective impurity implantation or diffusion periodically disorders GaInP and therefore modulates the d_{ij} matrix. The QPM period for the 1.5-μm light is approximately 2.5 μm.

$$d_{ij}^{(\mathrm{O:wg})} = \begin{bmatrix} 0 & 0 & 0 & 0 & d'_{15}+d'_{14} & \dfrac{d'_{33}-d'_{31}}{\sqrt{2}} \\ \dfrac{d'_{33}+d'_{31}-2d'_{15}}{\sqrt{2}} & \dfrac{d'_{33}+d'_{31}+2d'_{15}}{\sqrt{2}} & \sqrt{2}d'_{31} & d'_{15}-d'_{14} & 0 & 0 \\ d'_{31}+d'_{14} & d'_{31}-d'_{14} & d'_{33} & \sqrt{2}d'_{15} & 0 & 0 \end{bmatrix}, \quad (7)$$

or

$$d_{ij}^{(\mathrm{Mix:wg})} = \begin{bmatrix} 0 & 0 & 0 & 0 & d'_{15}+d'_{14} & 0 \\ 0 & 0 & 0 & d'_{15}-d'_{14} & 0 & 0 \\ d'_{31}+d'_{14} & d'_{31}-d'_{14} & d'_{33} & 0 & 0 & 0 \end{bmatrix}, \quad (8)$$

$$d_{ij}^{(\mathrm{DO:wg})} = \begin{bmatrix} 0 & 0 & 0 & 0 & d''_{14} & 0 \\ 0 & 0 & 0 & -d''_{14} & 0 & 0 \\ d''_{14} & -d''_{14} & 0 & 0 & 0 & 0 \end{bmatrix}, \quad (9)$$

which are now transformed into the ([1, 1, 0], [$\bar{1}$, 1, 0], [0, 0, 1]) waveguide frames (wg).

These results indicate that the [0, 0, 1]-TM-polarized fundamental is phase matched with the TM-polarized SH through the modulation of the (3.3) component, which varies between d'_{33} and zero. Note that for rectangular regions, the effective nonlinearity involved in using this form of on–off modulation for phase matching is given by d'_{33}/π. The fundamental TE mode polarized along [1, 1, 0] (or [$\bar{1}$, 1, 0]) is phase matched with the TM-polarized SH mode through modulation of the (3.1) component between $d'_{31}+d'_{14}$ and d''_{14}, yielding an effective nonlinearity of d'_{31}/π. We estimated the necessary QPM period for 1.5-μm light to be approximately 2.5 μm, based on the refractive indices at 1.5 μm and 0.775 μm.[11]

4. MAKER-FRINGE MEASUREMENTS

An experimental search for the order–disorder modulated coefficients (d'_{33}, d'_{31}, and d'_{15}) was performed by Maker-fringe techniques[25] with an incident fundamental at 1.579 μm (Fig. 4). The fundamental beam was generated by a Q-switched, seeded Nd:YAG laser, a KDP frequency doubler, and a H_2 Raman cell. A silicon window with a cutoff of 1.1 μm was used to filter out the laser and the doubled wavelengths. The pulse width was 11 ns, and the repetition rate was 10 Hz. Spatial filtering elements, a spatial filter (SF) and two lenses (L3 and L4), were carefully used to improve the 1.579-μm beam quality. The beam alignment with respect to the sample rotation axis, as well as the beam quality, were checked with an α-quartz reference to verify that the Maker fringes were symmetric for incidence angles up to 75°. The typical pulse energy used for the GaInP samples was 10 μJ. A monochromator was used to filter out the fundamental light. SH signals were detected by a photomultiplier tube and a boxcar integrator. Measured data were calibrated with respect to an α-quartz (d_{11} = 0.4 pm/V) reference.

Figure 5 shows the beam-sample geometry and our $Ga_{0.5}In_{0.5}P$ sample whose lattice constant matches that of GaAs. Only the ordered samples were investigated for

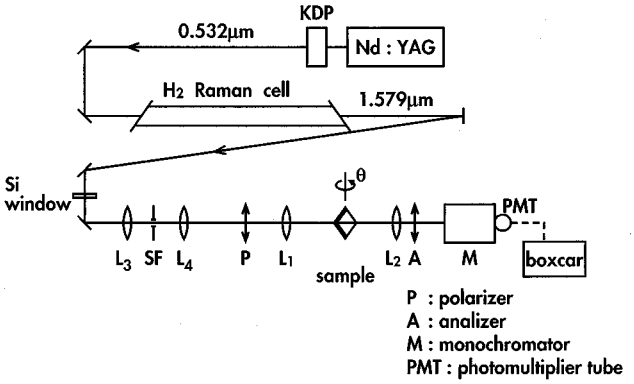

Fig. 4. Maker-fringe measurement setup at 1.579 μm. The pulse width was 11 ns, the repetition rate was 10 Hz, and the typical pulse energy used for GaInP samples was 10 mJ.

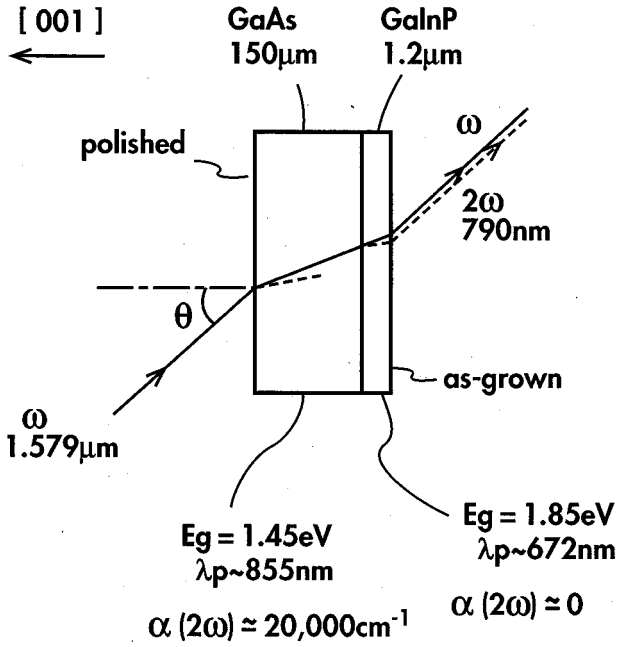

Fig. 5. $Ga_{0.5}In_{0.5}P$ sample structure, grown lattice matched on a (0, 0, 1) GaAs substrate by metallorganic vapor phase epitaxy. The GaInP thickness of 1.2 μm is close to the coherence length of 1.36 μm. After the growth, the GaAs substrate was wrapped and polished for the measurements.

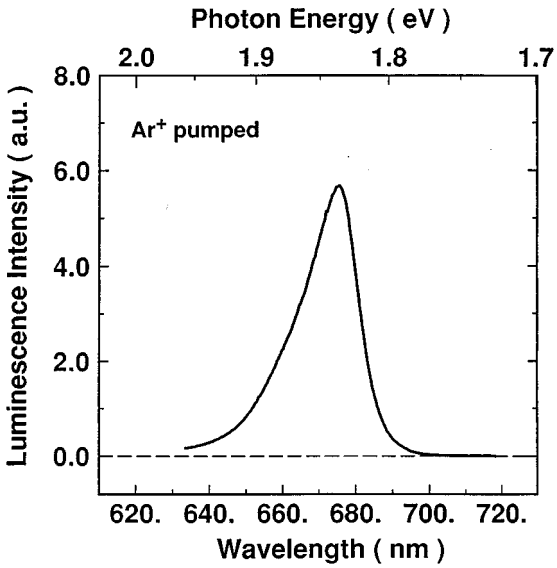

Fig. 6. Photoluminescence from our GaInP sample at room temperature shows the typical spectrum and a peak at 675 nm (1.84 eV).

reasons that will be obvious in Section 5. The GaInP layer was 1.2 μm thick and was grown undoped on a (0, 0, 1) GaAs substrate by metallorganic vapor phase epitaxy at 660 °C. The V/III ratio was 130, and growth speed was 1.8 μm/h. The crystal quality and Ga composition of our samples were tested by photoluminescence and double-crystal x-ray rocking curves. The luminescence from our samples (before and after the wrapping and the polishing processes) showed the usual spectrum with a peak at 0.675 μm (1.84 eV, Fig. 6). The x-ray rocking curve showed that the lattice constants were within $\pm 1 \times 10^{-3}$ with respect to the GaAs substrates. These data also ensure the Ga composition of our samples to be 0.49 ± 0.01. The degree of ordering δ ($0 \leqslant \delta \leqslant 0.5$) of our sample was approximately 0.2, as estimated from the difference in band-gap energy between this sample and that of disordered GaInP.[26]

The coherence lengths, $l_c \equiv \lambda/4(n_{2\omega} - n_\omega)$, at 1.579 μm for GaInP and GaAs, were estimated to be 1.36 μm and 1.52 μm, respectively. The 1.2-μm-thick GaInP sample was thus appropriate for the measurements because it was comparable to the coherence length. After the growth, the GaAs substrate was wrapped down to a thickness of 150 μm and polished to facilitate the focusing of the fundamental beam into it. Then the sample was cleaved into 5 mm $\times$ 5 mm or 10 mm $\times$ 10 mm sizes and glued onto the rotation stage.

The SHG projection factors for the domain-mixed GaInP crystal were determined (see Table 1) based on the $d_{ij}^{(\text{Mix: } T_d)}$ in Eq. (5). Although the d_{14} coefficient of the GaAs substrate could also generate the SH; these projection factors suggest that the modulatable components (d'_{33}, d'_{31}, and d'_{15}) of GaInP can be measured independently of the d_{14} components of GaAs and GaInP by use of $k \perp [100]$ configurations. It was also possible to avoid strong absorption of the 0.790-μm SH signal in the GaAs substrate ($E_g = 1.45$ eV, $\lambda = 855$ nm) by focusing the incident fundamental beam onto the GaInP through the polished GaAs surface (Fig. 5). Although the input does suffer some TPA in GaAs, the TPA propagation loss through the 150 μm GaAs was estimated to be negligible at our input intensity.

Regarding the analysis of the measured data needed to evaluate the modulatable components, we numerically confirmed that a procedure as simple as that used by Jerphagnon and Kurtz[25] is valid even for our two-layer sample structure for the following reasons: (i) The incoherent multireflections of the fundamental beam[27] between the GaInP and GaAs surfaces were negligible. They modified the results by less than 4%. (ii) The boundary conditions at the GaInP/GaAs interface could be neglected because the refractive indices were comparable. (iii) The approximation needed for defining the projection factors (Appendix B.2 in Ref. 25) was satisfied, even though Jerphagnon and Kurtz claimed that small dispersion (i.e., $n_\omega \approx n_{2\omega}$) in the test material is a necessary precondition. Thus we can analyze data as if we did not have the GaAs substrate beneath the GaInP crystal,

Table 1. Projection Factors for Domain-Mixed GaInP Crystals[a]

		2ω	
ω		TE	TM
$k \perp [100]$	TE	0	$d'_{31} \sin\theta'$
$k \perp [100]$	TM	$\pm 2d'_{14} \cos\theta' \sin\theta'$	$(d'_{31} + 2d'_{15}) \cos^2\theta' \sin\theta' + d'_{33} \sin^3\theta'$
$k \perp [110]$	TE	0	$(d'_{31} + d'_{14}) \sin\theta'$
$k \perp [110]$	TM	0	$(d'_{31} + 2d'_{15} \pm 3d'_{14}) \cos^2\theta' \sin\theta' + d'_{33} \sin^3\theta'$

[a] These factors are based on the $d_{ij}^{(\text{Mix:Td})}$. The θ' represents the incidence angle for the fundamental wave in the material. When the Kleinman's symmetry holds, d'_{15} equals d'_{31}. The [010] and [$\bar{1}$10] directions were equivalent to [100] and [110], respectively, regarding these factors.

Table 2. Material Parameters Used for the Analyses

	n_ω	$n_{2\omega}$	Thickness (μm)	α_ω (cm^{-1})	$\alpha_{2\omega}$ (cm^{-1})	Ref.
$Ga_{0.5}In_{0.5}P$	3.12	3.41	1.2	0	0	11
GaAs	3.43	3.69	150	0	20 000	28
α-quartz	1.5276	1.5389	1000	0	0	29

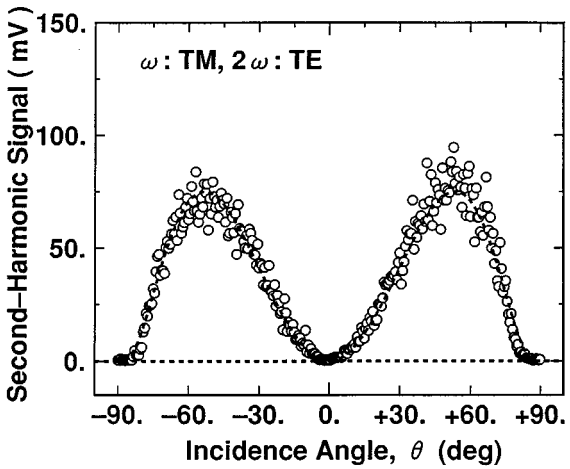

Fig. 7. Measured TE-polarized d_{14} signal obtained by focusing the TM-polarized fundamental beam. The d'_{14} coefficient of GaInP was calculated as 110 pm/V, assuming a d''_{14} of 130 pm/V in GaAs[6] and a linear absorption coefficient of 20 000 cm^{-1} for the SH wave in GaAs.

except for contributions from the d_{14} coefficient. Material parameters used in the analyses are given in Table 2.

5. RESULTS AND DISCUSSION

A strong SH effect owing to the d'_{14} coefficient of GaInP was clearly observed in the Maker-fringe data. The results for the TE-polarized SH signal in Fig. 7 were obtained for a TM-polarized input. They show the interference between the SH fields generated by d_{14} in GaAs and d'_{14} in GaInP. Because the GaInP-film thickness is comparable to the effective depth from which the GaAs SH signal is expected, as calculated from the linear GaAs absorption coefficient of 20 000 cm^{-1}, the GaInP and the GaAs SH signals are comparable in magnitude. This produces interference between them as the sample is rotated and the effective SH radiating thickness of the film increased. Assuming a value of d_{14} of 130 pm/V for GaAs,[6] the d'_{14} coefficient of GaInP was deduced to be 110 pm/V. As discussed in Section 2, this value is comparable to that of GaAs, as expected on physical grounds.

The beam-sample geometry for measuring d'_{33}, taken from Table 1, was a fundamental and a harmonic that are both TM polarized. Figure 8 shows the data as a function of the external incidence angle θ (θ' in Table 1 is the internal angle of incidence). The circles represent the measured SH signals obtained by setting the polarizer and the analyzer along the TM direction as accurately as possible. Assuming the angular dependence for d'_{33} in Table 1 (signal $\propto |d'_{33} \sin^3 \theta'|^2$), and a nonlinearity of 60 pm/V (chosen to produce approximately the observed peak), the theoretical curve (solid curve in Fig. 8) is quite dissimilar from the data in two ways: one, the functional dependence on θ is wrong, and two, there is a nonzero signal at $\theta = 0$. This means that the data are not dominated by d'_{33}. In fact, including the two other contributing coefficients d'_{31} and d'_{15} does not solve these problems (dotted curve). Therefore we conclude that there is a large, unwanted contribution from another coefficient. The only reasonable choice is d'_{14}.

In a separate set of experiments we found that the measurement of the modulatable components was limited by a surprisingly strong SH-signal dependence on the polarizer and analyzer directions. This effect is not obvious and merits further discussion. It has its origin in the large magnitude of the d_{14} and d'_{14} components of both GaAs and GaInP, respectively, the orientation of the crys-

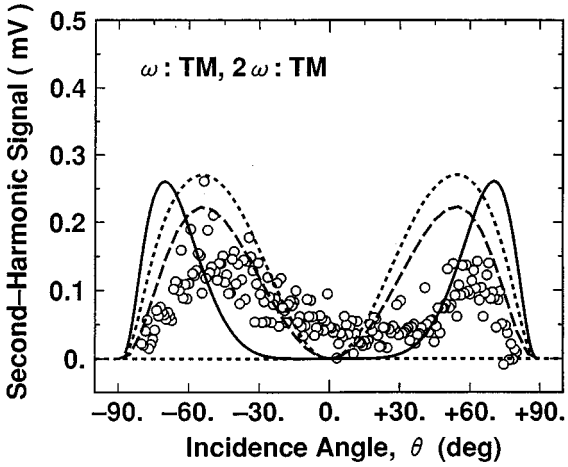

Fig. 8. Measured SH signals obtained by setting the polarizer and analyzer along the TM direction. The solid curve shows a simulated d'_{33} signal assuming $d'_{33} = 60$ pm/V. Coexistence of a $d'_{31} + 2d'_{15}$ component changes the signal shape. For example, the dotted curve shows a simulated signal assuming both $d'_{31} + 2d'_{15} = -2.9$ pm/V and $d'_{33} = 34$ pm/V, which is not distinguishable from d'_{14} leakage (dashed curve) assuming only a 1° misfit ($\psi_{1,2} = 1°$). Thus our detection limit for the d'_{33} coefficient was approximately 60 pm/V.

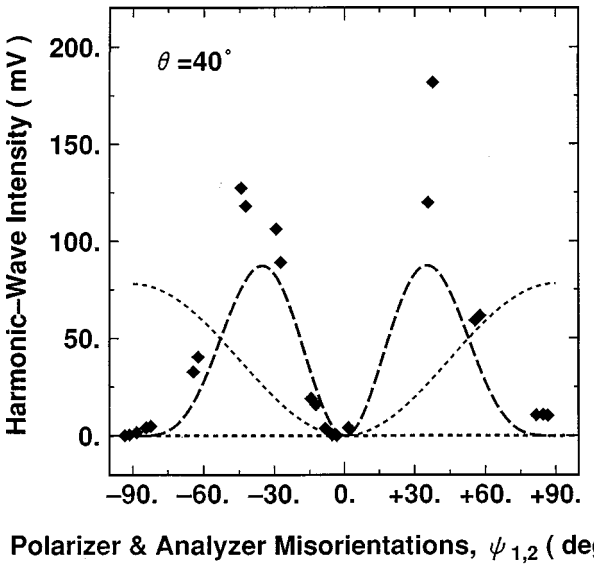

Fig. 9. Signal intensities measured at a fixed incidence angle (θ) of 40° obtained by rotating the polarizer (ψ_1) and the analyzer (ψ_2) synchronously (i.e., $\psi_1 = \psi_2 = \psi_{1,2}$). The calculated d'_{14} signal (dashed curve) reproduced well both the magnitude and shape of the measured data. This d'_{14} signal leakage in the vicinity of $\psi_{1,2} = 0$ was much stronger than we had originally expected (dotted curve).

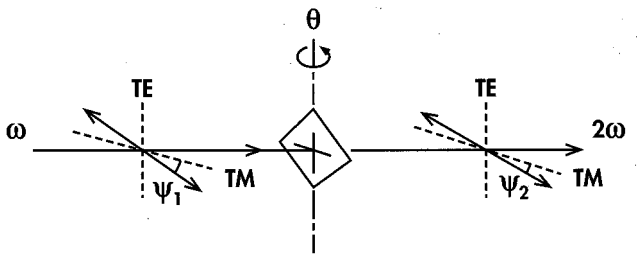

Fig. 10. Polarizer (ψ_1) and analyzer (ψ_2) rotations with respect to the sample axis.

tal film, and the limited range of incidence angles within the sample. To clarify this polarization problem, we measured the signal variation induced by intentionally rotating the polarizer and analyzer and compared the result with calculations. The squares in Fig. 9 show the signal intensities measured at a fixed incidence angle (θ) of 40°, obtained by rotating the polarizer (ψ_1) and the analyzer (ψ_2) together (i.e., $\psi_1 = \psi_2 = \psi_{1.2}$) with respect to the sample axis (Fig. 10). By definition, a signal at $\psi_{1.2} = 0$ corresponds to the TM-polarized SH generated by a TM-polarized fundamental. At $\psi_{1.2} = 90°$, a TE-polarized SH signal is obtained with a TE-polarized fundamental. Also calculated was the SH signal as a function of arbitrary $\psi_{1.2}$, based on the measured d'_{14} value. Note that the calculated data (dashed curve) reproduced both the magnitude and the shape of the measured data.

The strong d'_{14} signal in the vicinity of $\psi_{1.2} = 0$ limited the experimental measurement sensitivity for modulatable components such as d'_{33}. The above examination clarified that this limitation is much stronger than we had expected. Initially we had expected the SHG signal owing to d'_{14} to be of order $S(d'_{14})\sin^2\psi_{1.2}$ (dotted curve) in the vicinity of $\psi_{1.2} = 0$, where $S(d'_{14})$ ($\propto|2d'_{14}\cos\theta'\sin\theta'|^2$) represents the peak intensity of the TE-polarized signal originating from d'_{14}, generated by a TM-polarized fundamental. We had not anticipated that the SH signals from d'_{14} would be so much stronger than those from the modulatable coefficients.

The data in Fig. 8 was used to obtain an upper limit for d'_{33}. The solid curve shows a simulated d'_{33} signal ($|d'_{33}\sin^3\theta'|^2$) assuming a d'_{33} of 60 pm/V. The dotted curve shows a simulated TM-polarized signal ($|(d'_{31} + 2d'_{15})\cos^2\theta'\sin\theta' + d'_{33}\sin^3\theta'|^2$) assuming $d'_{31} + 2d'_{15} = -2.9$ pm/V and a d'_{33} of 34 pm/V. (Both of these combinations were chosen to reproduce approximately the observed peaks.) Because of the change in sign on either side of $\theta = 0$ for the $d'_{31} + 2d'_{15}$ contribution, this term interferes destructively with the d'_{33} component and thus changes the signal shape and shifts the peak positions. On the other hand, the dashed curve shows a simulated d'_{14} leakage signal assuming only a 1° misalignment relative to the crystal axis ($\psi_{1.2} = 1°$). These simulations indicate the experimental problem that a d'_{33} of 34 pm/V is not distinguishable from a d'_{14} leakage signal, although the measured data imply that our experimental accuracy was less than 1°. Considering the fact that the independent variables d'_{33} and $d'_{31} + 2d'_{15}$ interfere with each other, we estimate that a d'_{33} as large as 60 pm/V might not be measurable here. Thus we set our detection limit for the d'_{33} coefficient as approximately 60 pm/V. This value is relatively large when compared with the phase-matchable d_{ij} of other relevant nonlinear materials. Therefore our results neither confirm nor rule out the potential of this material for QPM.

Similar problems were experienced in measurements aimed at evaluating d'_{31} with TM-polarized signals ($|d'_{31}\sin\theta'|^2$) generated by a TE-polarized fundamental. Repeating the procedures just discussed, we estimated an upper limit for the d'_{31} coefficient of 20 pm/V. Although these detection limits for d'_{33} and d'_{31} are experimentally inevitable, as proved above given the sample geometry and technique used, they are unexpectedly large when compared with a d'_{14} of 110 pm/V.

The difficulty discussed above comes partly from the crystal orientation of our samples. Ordered GaInP crystals having surfaces perpendicular to the $[\bar{1}, 1, 1]$ crystal axis would improve the detection sensitivity. However, it has proven technically impossible to form the ordered GaInP crystal on a $[\bar{1}, 1, 1]$ surface of the GaAs substrate because only disordered crystals have been grown on the $[\bar{1}, 1, 1]$ surface.[30] So, an ordered GaInP lattice structure on the $[\bar{1}, 1, 1]$ surface would need to be grown artificially, for example, by growth of a $(GaP)_1(InP)_1$ superlattice with an atomic-layer epitaxy technique.

Another approach, which could potentially yield a method to measure those coefficients needed for QPM, would be to use a modulation-detection technique for samples on the previously discussed [0, 0, 1] surface. By modulation of the analyzer polarization in various ways (i.e., modulation of the linear-polarization direction, modulation between linear and elliptical polarizations, etc.) at a frequency ω_m, the components of the detected signals at the frequency ω_m would be related to the d_{ij} coefficients differently than in Table 1. Table 3 shows examples of the signal components at ω_m for the case in which the linear-polarization direction of the analyzer is modulated around either the TM- or TE-polarization direction. The ω_m frequency components are either zero or

Table 3. Modulation Detection Signals[a]

		2ω	
ω		TE	TM
$k\perp[100]$	TE	0	0
$k\perp[100]$	TM	$4[(d'_{31} + 2d'_{15})\cos^2\theta' + d'_{33}\sin^2\theta']d'_{14}\cos\theta'\sin^2\theta'$	$4[(d'_{31} + 2d'_{15})\cos^2\theta' + d'_{33}\sin^2\theta']d'_{14}\cos\theta'\sin^2\theta'$
$k\perp[110]$	TE	0	0
$k\perp[110]$	TM	0	0

[a] These forms correspond to absolute squares of projection factors.

proportional to $d'_{33}d'_{14}$ whenever d'_{33} is involved. Combining this with the measurements for d'_{14} reported here, this modulation scheme should improve the detection limit on d'_{33}; even if the d'_{14} contribution to the intensity owing to polarization misalignments is of the order of $|d'_{14}|^2$, the signal-to-noise ratio is improved to

$$\frac{O(|d'_{33}d'_{14}|)}{O(|d'_{14}|^2)} = \frac{O(|d'_{33}|)}{O(|d'_{14}|)}, \tag{10}$$

as compared with the previous case, which is proportional to

$$\frac{O(|d'_{33}|^2)}{O(|d'_{14}|^2)}. \tag{11}$$

Further studies along these lines are anticipated.

6. CONCLUSION

The $\chi^{(2)}$ properties of ordered GaInP thin-film crystals having $C_{3\nu}(3m)$ symmetry were studied theoretically and experimentally. It was shown theoretically that this material has the potential for realizing quasi-phase-matched waveguides. Only well-established processes, such as photolithographic patterning, impurity implantation, etc., are required for quasi-phase-matched waveguide fabrication. The possible d_{ij} modulation for QPM is between d'_{33} (for $C_{3\nu}$ GaInP) and zero (for cubic GaInP) for the (3.3) component and between $d'_{31} + d'_{14}$ (for $C_{3\nu}$ GaInP) and d''_{14} (for cubic GaInP) for the (3.1) component. The coefficients that can be changed by disordering (d'_{33}, d'_{31}, and d'_{15}) are physically related to the $C_{3\nu}$ crystal distortion, while the d'_{14} is a property of the original cubic crystal.

Experiments were performed on ordered, 1.2-μm-thick $Ga_{0.5}In_{0.5}P$ samples epitaxially grown on GaAs substrates to measure the d_{ij} coefficients at 1.5 μm. Only the d'_{14} = 110 pm/V coefficient was measured. It was shown that SH signals originating from d'_{14} contaminated the measurements of the other coefficients because of slight misorientations of the polarizer–analyzer pair. Upper limits of 60 pm/V for d'_{33} and 20 pm/V for d'_{31} were found for misalignments of only 1°. Possible future experiments to improve these limits were discussed.

ACKNOWLEDGMENTS

We acknowledge John Sipe, Y. Wang, W. E. Torruellas, and N. Bloembergen for discussions. We also thank Kunihiro Hara for wrapping and polishing samples. Y. Ueno thanks Ikuo Mito for his continuous encouragement.

*Present address: Opto-Electronics Research Laboratories, NEC Corporation, 34 Miyukigaoka, Tsukuba, Ibaraki 305, Japan. E-mail: ueno@obl.cl.nec.co.jp

REFERENCES AND NOTES

1. R. DeSalvo, D. J. Hagan, M. Sheik-Bahae, G. I. Stegeman, and E. W. Van Stryland, "Self-focusing and self-defocusing by cascaded second-order effects in KTP," Opt. Lett. **17**, 28–30 (1992).
2. G. I. Stegeman, M. Sheik-Bahae, E. Van Stryland, and G. Assanto, "Large nonlinear phase shifts in second-order nonlinear-optical processes," Opt. Lett. **18**, 13–15 (1993).
3. M. L. Sundheimer, Ch. Bosshard, E. W. Van Stryland, G. I. Stegeman, and J. D. Bierlein, "Large nonlinear phase modulation in quasi-phase-matched KTP waveguides as a result of cascaded second-order processes," Opt. Lett. **18**, 1397–1399 (1993).
4. R. Schiek, M. L. Sundheimer, D. Y. Kim, Y. Baek, G. I. Stegeman, H. Seibert, and W. Sohler, "Direct measurement of cascaded nonlinearity in lithium niobate channel waveguides," Opt. Lett. **19**, 1949–1951 (1994).
5. See, e.g., L. E. Myers, R. C. Eckardt, M. M. Fejer, R. L. Beyer, W. R. Bosenberg, and J. W. Pierce, "Quasi-phase-matched optical parametric oscillators in bulk periodically poled $LiNbO_3$," J. Opt. Soc. Am. B **12**, 2102–2116 (1995).
6. S. Singh, "Second-harmonic coefficients," in *CRC Handbook of Laser Science and Technology*, M. J. Weber, ed. (CRC Press, Boca Raton, Fla., 1986), Vol. 3, Part 1, p. 88, Table 1.1.16.
7. J. Khurgin, "Second-order nonlinear effects in asymmetric quantum-well structures," Phys. Rev. B **38**, 4056–4066 (1988); C. Kelaidis, D. C. Hutchings, and J. M. Arnold, "Asymmetric two-step GaAlAs quantum well for cascaded second-order processes," IEEE J. Quantum Electron. **30**, 2998–3005 (1994).
8. M. J. Angell, R. M. Emerson, J. L. Hoyt, J. F. Gibbons, L. A. Eyres, M. L. Bortz, and M. M. Fejer, "Growth of alternating ⟨100⟩/⟨111⟩-oriented II–VI regions for quasi-phase-matched nonlinear optical devices on GaAs substrates," Appl. Phys. Lett. **64**, 3107–3109 (1994); S. J. Yoo, R. Bhat, C. Caneau, and M. A. Koza, "Quasi-phase-matched second-harmonic generation in AlGaAs waveguides with periodic domain inversion achieved by wafer-bonding," Appl. Phys. Lett. **66**, 3410–3412 (1995).
9. A. Gomyo, T. Suzuki, and S. Iijima, "Observation of strong ordering in $Ga_xIn_{1-x}P$ alloy semiconductors," Phys. Rev. Lett. **60**, 2645–2648 (1988); A. Gomyo, T. Suzuki, K. Kobayashi, S. Kawata, and I. Hino, "Evidence for the existence of an ordered state in $Ga_{0.5}In_{0.5}P$ grown by metalorganic vapor phase epitaxy and its relation to band-gap energy," Appl. Phys. Lett. **50**, 673–675 (1987); O. Ueda, M. Takikawa, J. Komeno, and I. Umebu, "Atomic structure of ordered InGaP crystals on (0,0,1) GaAs substrates by metalorganic chemical vapor deposition," Jpn. J. Appl. Phys. **26**, L1824–L1827 (1987).
10. Y. Ueno, H. Fujii, H. Sawano, K. Kobayashi, K. Hara, A. Gomyo, and K. Endo, "30-mW 690-nm high-power strained-quantum-well AlGaInP laser," IEEE J. Quantum Electron. **29**, 1851–1856 (1993).
11. H. Tanaka, Y. Kawamura, and H. Asahi, "Refractive indices of $In_{0.49}Ga_{0.51-x}Al_xP$ lattice matched to GaAs," J. Appl. Phys. **59**, 985–986 (1986).
12. A. Mascarenhas, S. Kurtz, A. Kibbler, and J. M. Olson, "Polarized band-edge photoluminescence and ordering in $Ga_{0.52}In_{0.48}P$," Phys. Rev. Lett. **63**, 2108–2111 (1989).
13. H. Fujii, Y. Ueno, A. Gomyo, K. Endo, and T. Suzuki, "Observation of stripe-direction dependence of threshold current density for AlGaInP laser diodes with CuPt-type natural superlattice in $Ga_{0.5}In_{0.5}P$ active layer," Appl. Phys. Lett. **61**, 737–739 (1992); Y. Ueno, "Oscillator strength enhancement for [110]-polarized light in compressively strained GaInP ordered crystals used in AlGaInP laser," Appl. Phys. Lett. **62**, 553–555 (1993).
14. A. Moritz, R. Wirth, C. Geng, F. Scholz, and A. Hangleiter, "Birefringence and tilted modes in ordered GaInP/AlGaInP waveguides and lasers," Appl. Phys. Lett. **68**, 1217–1219 (1996).
15. Y. Kostoulas, K. B. Ucer, G. W. Wicks, and P. M. Fauchet, "Femtosecond carrier dynamics in low-temperature grown $Ga_{0.5}In_{0.5}P$," Appl. Phys. Lett. **67**, 3756–3758 (1995).
16. Y. Ueno, K. Endo, H. Fujii, K. Kobayashi, K. Hara, and T. Yuasa, "Continuous-wave high-power (75 mW) operation of

a transverse-mode stabilized window structure 680-nm AlGaInP visible laser diode," Electron. Lett. **26**, 1726–1727 (1990); Y. Hämisch, R. Steffen, P. Röntgen, and A. Forchel, "Implantation induced order-disorder transition in $Ga_{0.52}In_{0.48}P/(Al_{0.35}Ga_{0.65})_{0.5}In_{0.5}P$ heterostructures," Jpn. J.Appl. Phys. **32**, L1492–L1495 (1993).

17. Y. Ueno, V. Ricci, and G. I. Stegeman, "Phase-matchable second-order susceptibility of GaInP crystals at 1.5-μm," *7th Topical Meeting of the European Optical Society*, Vol. 7 of EOS Topical Meetings Digest Series (European Optical Society, Orsay, France, 1996), pp. 185–186; V. Ricci, Y. Ueno, and G. I. Stegeman, "Measurement of the second-order susceptibility of GaInP films at 1.5 μm," in *Quantum Electronics and Laser Science Conference (QELS'96)*, Vol. 10 of 1996 OSA Technical Digest Series (Optical Society of America, Washington, D.C., 1996), pp. 21–22.
18. E. Ghahramani, D. J. Moss, and J. E. Sipe, "Full-band-structure calculation of first-, second-, and third-harmonic optical response coefficients of ZnSe, ZnTe, and CdTe," Phys. Rev. B **43**, 9700–9710 (1991).
19. See, e.g., F. A. Hopf and G. I. Stegeman, *Applied Classical Electrodynamics* (Wiley, New York, 1986), Vol. 2, p. 14; R. W. Boyd, *Nonlinear Optics* (Academic, Boston, 1992), p. 46.
20. T_d crystals have three IC_4 axes and four C_3 axes. Because of the Ga–In ordering, ordered GaInP loses all IC_4 axes and three of the four C_3 axes, which causes symmetry breakdown to $C_{3\nu}$.
21. T. Kurimoto and N. Hamada, "Electronic structure of the $(GaP)_1/(InP)_1$ (111) strained-layer superlattice," Phys. Rev. **40**, 3889–3895 (1989).
22. Domain-mixed ordered GaInP crystal has been used as the active layer for the above-mentioned red lasers in Ref. 10. Thus the domain-mixed crystal is supposed to be stable, even under a high-density carrier injection of approximately 2 kA/cm^2.
23. The volume of the one domain equals that of the other, because these two domains are equivalent with respect to the (001) surface. In contrast, the one domain dominates the other when grown on surfaces tilted from (001). Refer to A. Gomyo, T. Suzuki, K. Kobayashi, S. Kawata, H. Hotta, and I. Hino, "Effects of GaAs-substrate surface misorientation from (001) on band-gap energy in $Ga_{0.5}In_{0.5}P$," NEC Res. Dev. **35**, 134–143 (1994).
24. $C_{3\nu}$ GaInP has one C_3 axis and three σ_ν planes for symmetry operations. The average owing to the domain mixture causes the crystal to lose the C_3 axis and two of the three σ_ν planes and to gain a new $(\bar{1}, 1, 0)$ σ_ν plane and one [0, 0, 1] C_2 axis. The (1, 1, 0) σ_ν plane remains. Consequently, a set of symmetry operations with one C_2 axis and two σ_ν planes corresponds to the $C_{2\nu}$ symmetry.
25. J. Jerphagnon and S. K. Kurtz, "Maker fringes: a detailed comparison of theory and experiment for isotropic and uniaxial crystals," J. Appl. Phys. **41**, 1667–1681 (1970).
26. P. Ernst, C. Geng, F. Scholz, and H. Schweizer, "Band-gap reduction and valence-band splitting of ordered $GaInP_2$," Appl. Phys. Lett. **67**, 2347–2349 (1995).
27. In a few measurements we observed sharp Fabry–Perot fringes corresponding to the distance of 150 μm between GaInP and GaAs surfaces, in addition to Maker fringes, which correspond to the GaInP thickness of 1.2 μm. In most of our measurements, however, the fundamental lights are believed to be incoherently multireflected between GaInP and GaAs surfaces.
28. D. E. Aspens, S. M. Kelso, R. A. Logan, and R. Bhat, "Optical properties of $Al_xGa_{1-x}As$," J. Appl. Phys. **60**, 754–767 (1986).
29. V. G. Dmitriev, G. G. Gurzadyan, and D. N. Nikogosyan, eds., *Handbook of Nonlinear Optical Crystals* (Springer-Verlag, Berlin, 1991).
30. A. Gomyo, T. Suzuki, S. Iijima, H. Hotta, H. Fujii, S. Kawata, K. Kobayashi, Y. Ueno, and I. Hino, "Nonexistence of long-range order in $Ga_{0.5}In_{0.5}P$ epitaxial layers grown on (111)B and (110)GaAs substrates," Jpn. J. Appl. Phys. **27**, L2370–L2372 (1988).